Mode Coupling in Coaxial Waveguides with Varying-Radius Center and Outer Conductors

Jamal Shafii, *Student Member, IEEE,* and Ronald J. Vernon, *Member, IEEE*

***Abstract*—The mode conversion process in a coaxial waveguide with varying-radius center and outer conductors is shown to be described by a system of first-order differential equations—the coupled mode equations. The nondiagonal coefficients of this system are called the coupling coefficients. In this paper, we derive the explicit expressions for the coupling coefficients in a varying-radius coaxial waveguide and discuss some of their important features. These coefficients can be used in determining model conversion in a coaxial cavity with slowly varying walls or designing and analyzing coaxial waveguide tapers and mode converters. Some experimental results of the coupling coefficients for the case of azimuthally symmetric modes, TE_{0n} modes, are also given.**

I. Introduction

GYROTRONS have been used to heat magnetically confined plasmas encountered in fusion research at the electron-cyclotron-resonance frequency. High-power millimeter-wave gyrotrons have recently been designed with highly overmoded coaxial resonators [1], [2]. It has been shown that the inclusion of an inner conductor in the gyrotron's cavity can reduce mode competition and hence may lead to more stable operation in the desired mode in the cavity by moving the resonant frequencies of competing modes [1], [3].

It is important to examine mode conversion in overmoded coaxial waveguide cavity resonators with a varying-radius wall profile. It will also be required to taper the diameter of the outer and/or center conductor with negligible mode conversion outside the cavity (but within the tube) [4]. It may also be desirable that the cavity's output mode be converted into a different mode by means of one or more coaxial mode converters.

In this paper, we derive the coupling coefficients and discuss mode coupling in overmoded coaxial waveguides with varying-radius center- and outer-conductor profiles. By an overmoded waveguide, we mean a waveguide whose cross section is large enough such that, in addition to the TEM mode, higher-order modes can also propagate. The material in this paper is an extension of work briefly reported by Shafii and Vernon in 1992 [5].

We represent the fields at any cross section of the nonuniform coaxial waveguide as a superposition of the fields of the eigenmodes of a uniform coaxial guide of the same cross section. The amplitudes of these eigenmodes depend on the coordinate along the axis of the varying-radius guide. From Maxwell's equations, the mode amplitudes are shown to be described by a system of first-order ordinary differential equations. The coefficients of this system are called the coupling coefficients.

This method of derivation of the coupling coefficients is sometimes called the method of cross sections [8], [10]. This method has been used in analyzing mode coupling in hollow waveguides with different types of wall irregularities such as waveguides with a varying-radius wall profile for the case of azimuthally symmetric transverse electric modes [6], [7], corrugated waveguides with varying corrugation depth and diameter change [8], [9], acoustic waveguides [10], and curved waveguides of constant cross section with varying curvature and filled with an inhomogeneous material [11].

In Section II of this paper, the integral expression for the coupling coefficients is discussed. (In Appendix I, a brief derivation of the integral expression is given.) In Section III, an alternative expression for the coupling coefficients is given which consists of line integrals of the fields of the normal modes along the boundary of the waveguide cross section. In Section IV, the normal-mode fields of a uniform circular coaxial guide are presented. These normal-mode fields are used to derive the explicit formulas for the coupling coefficients in Section V. In Section VI, the validity of the method of cross sections is discussed. Some numerical and experimental results are presented in Sections VII and VIII, respectively.

II. The Integral Expressions for the Coupling Coefficients in a Varying-Radius Coaxial Waveguide

We assume that the axis of the nonuniform waveguide coincides with the z-axis of the cylindrical coordinate system ρ, ϕ, and z, and that the guide is homogeneously filled with isotropic, lossless matter, the plane wave number of which is

$$k = \omega\sqrt{\mu\epsilon} \tag{1}$$

where μ and ϵ are, respectively, the permeability and the permittivity of the medium inside the guide. The time variation is taken to be $e^{j\omega t}$. The walls of the guide are taken to be of perfect conductor. Hence, the coupling mechanism is nondissipative. (Coupling due to ohmic wall losses are normally negligible compared to coupling due to wall distortions in guides fabricated from good conductors.)

The boundary conditions on the electric field $\boldsymbol{E}$ and the magnetic field $\boldsymbol{H}$ at the outer wall of the guide are

$$E_\phi = 0 \tag{2a}$$

$$E_z + E_\rho \tan\theta = 0 \tag{2b}$$

$$H_\rho - H_z \tan\theta = 0 \tag{2c}$$

Manuscript received September 1, 1993; revised June 21, 1994. This work was supported by the U.S. Department of Energy under Contract DE-FG02-85ER52122.

The authors are with the Department of Electrical and Computer Engineering, University of Wisconsin, Madison, WI 53706 USA.

IEEE Log Number 9407444.

where θ is the angle that the tangent line to the outside wall makes with the z-axis. The boundary conditions at the center-conductor wall likewise become

$$E_\phi = 0 \tag{3a}$$

$$E_z + E_\rho \tan\psi = 0 \tag{3b}$$

$$H_\rho - H_z \tan\psi = 0 \tag{3c}$$

where ψ is the angle that the tangent line to the center-conductor wall makes with the z-axis.

We consider some cross section of the nonuniform waveguide $S = S_o$ at $z = z_o$, as illustrated in Fig. 1, and construct a uniform waveguide with the same local cross section S_o. We then expand the fields of the nonuniform guide at the cross section S_o in terms of the normalized fields of the modes of the uniform guide as follows:

$$\boldsymbol{E}_t = \sum_\tau V_\tau(z)\tilde{\boldsymbol{e}}_{t\tau}(\rho, \phi) \tag{4a}$$

$$E_z = \sum_\tau v_\tau(z)\tilde{e}_{z\tau}(\rho, \phi) \tag{4b}$$

$$\boldsymbol{H}_t = \sum_\tau I_\tau(z)\tilde{\boldsymbol{h}}_{t\tau}(\rho, \phi) \tag{4c}$$

$$H_z = \sum_\tau i_\tau(z)\tilde{h}_{z\tau}(\rho, \phi). \tag{4d}$$

Here, $\tilde{\boldsymbol{e}}_\tau(\rho, \phi)$ and $\tilde{\boldsymbol{h}}_\tau(\rho, \phi)$ are only functions of the transverse coordinates. The nonnegative integers τ or ν are used as indices for the eigenmodes. Furthermore, the subscripts t and z, respectively, denote the transverse and the $z-$directed components of the fields. The "$\sim$" over the functions in (4) indicates that these functions are normalized such that they satisfy the orthogonality relations given below

$$\int\int_{S_o} \tilde{\boldsymbol{e}}_{t\tau} \cdot \tilde{\boldsymbol{e}}^*_{t\nu}\, dS = \delta_{\tau\nu} \tag{5a}$$

$$\int\int_{S_o} \tilde{\boldsymbol{h}}_{t\tau} \cdot \tilde{\boldsymbol{h}}^*_{t\nu}\, dS = \delta_{\tau\nu} \tag{5b}$$

$$\int\int_{S_o} \tilde{e}_{z\tau}\tilde{e}^*_{z\nu}\, dS = \delta_{\tau\nu} \tag{6a}$$

$$\int\int_{S_o} \tilde{h}_{z\tau}\tilde{h}^*_{z\nu}\, dS = \delta_{\tau\nu} \tag{6b}$$

where superscript $*$ denotes the complex conjugate. Due to the normalization relation (5), the complex power flow in each mode τ is $P_\tau = V_\tau I^*_\tau$. The series expansion (4) does not converge uniformly. For example, $\tilde{e}_{z\tau}$ vanishes at the walls of the guide but according to (2b) or (3b), E_z doe not. This same argument also applies for the series expansion H_ρ. It is shown in Appendix I that the coupled differential equations are valid even though the field representation (4) is not uniformly convergent at the walls of the guide. The infinite series in (4) converges in the mean-square sense.

Let A^+_ν and A^-_ν be, respectively, the normalized complex amplitudes of the forward and backward propagating mode ν at $S = S_o$. We then have the following relations:

$$V_\nu = \sqrt{Z_\nu}(A^+_\nu + A^-_\nu) \tag{7a}$$

$$I_\nu = \frac{1}{\sqrt{Z_\nu}}(A^+_\nu - A^-_\nu). \tag{7b}$$

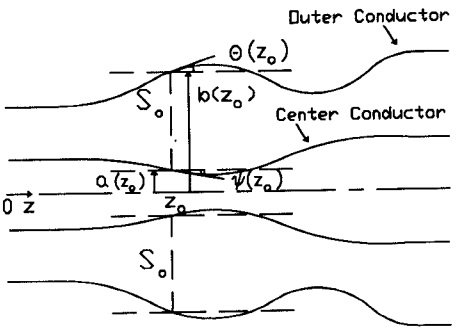

Fig. 1. The profile of a coaxial waveguide with varying-radius center and outer conductors.

The power transported in the $+\hat{\boldsymbol{a}}_z$ direction by the ν th mode is given by $|A^+_\nu|^2$, and than in the $-\hat{\boldsymbol{a}}_z$ direction by $|A^-_\nu|^2$. Here, Z_ν is the transverse mode impedance of the mode with index ν. As shown in the Appendix, the amplitudes of propagating modes are described by the following system of ordinary differential equations:

$$\frac{dA^+_\nu}{dz} = -j\beta_\nu A^+_\nu + \sum_\tau \kappa^+_{\nu\tau}A^+_\tau + \sum_\tau \kappa^-_{\nu\tau}A^-_\tau \tag{8a}$$

$$\frac{dA^-_\nu}{dz} = +j\beta_\nu A^-_\nu + \sum_\tau \kappa^-_{\nu\tau}A^+_\tau + \sum_\tau \kappa^+_{\nu\tau}A^-_\tau \tag{8b}$$

where β_ν is the propagation constant of the mode ν in the uniform waveguide with the cross section S_o. The coupling coefficients $\kappa^\pm_{\nu\tau}$ are given by

$$\kappa^\pm_{\nu\tau} = \frac{1}{2}\left(C_{\nu\tau}\sqrt{\frac{Z_\tau}{Z_\nu}} \mp C^*_{\tau\nu}\sqrt{\frac{Z_\nu}{Z_\tau}}\right), \qquad \nu \neq \tau \tag{9}$$

$$\kappa^+_{\nu\nu} = \frac{1}{2}(C_{\nu\nu} - C^*_{\nu\nu}) \tag{10}$$

$$\kappa^-_{\nu\nu} = \frac{1}{2}(C_{\nu\nu} + C^*_{\nu\nu}) - \frac{1}{2}\frac{1}{Z_\nu}\frac{dZ_\nu}{dz}. \tag{11}$$

Here the $C_{\nu\tau}$ is given by

$$C_{\nu\tau} = \int\int_{S_o} \tilde{\boldsymbol{e}}_{t\tau} \cdot \frac{\partial}{\partial z}\tilde{\boldsymbol{e}}^*_{t\nu}\, dS \tag{12}$$

where the integral is taken over the waveguide cross section S_o.

III. Alternative Formulas for the Coupling Coefficients

Since the dielectric material inside the coaxial guide has been taken to be homogeneous, coupling between modes occurs only due to the variation in the geometry of the waveguide walls. Hence, the coupling coefficients (9)–(12) given in the last section may be expressed by line integrals of the fields of the normal modes along the boundary of the waveguide cross section as shown below.

We write the vector eigenfunction $\tilde{\boldsymbol{e}}_{t\tau}$ of the normal modes in terms of the transverse gradient of a scalar potential function as

$$\tilde{\boldsymbol{e}}_{t\tau} = \hat{\boldsymbol{a}}_z \times \nabla_t \Psi_\tau \tag{13}$$

for TE_τ modes and

$$\tilde{\boldsymbol{e}}_{t\tau} = -\nabla_t \Psi_\tau \tag{14}$$

for TM_τ modes and the TEM mode [12]. Then we apply Stoke's theorem and Green's first identity in two dimensions to the waveguide cross section, and use the scalar Helmholtz equation for the scalar potential function

$$\nabla_t^2 \Psi_\tau + k_\tau^2 \Psi_\tau = 0 \tag{15}$$

and various orthogonality and boundary conditions on the potential function [12]. Furthermore, by using the following identities at the wall of the outer conductor:

$$\frac{\partial}{\partial z}\frac{\partial \Psi_\tau}{\partial \rho} \equiv -\frac{\partial^2 \Psi_\tau}{\partial \rho^2}\tan\theta \tag{16}$$

for TE_τ modes and

$$\frac{\partial \Psi_\tau}{\partial z} = -\frac{\partial \Psi_\tau}{\partial \rho}\tan\theta \tag{17}$$

for TM_τ modes [13] and similar identities at the wall of the center conductor by replacing θ with ψ, we obtain the following expressions for the coupling coefficients in terms of the fields of the power normalized modes along the boundary of the coaxial guide cross section.

The coupling coefficients between TE_ν and TE_τ modes are

$$\kappa_{\nu\tau}^{\pm} = \frac{1}{2}\frac{1}{\beta_\nu \mp \beta_\tau}\left[\oint_o \tan\theta(\omega\mu h_{z\tau}h_{z\nu}^* \cdot \pm\omega\mu h_{\phi\tau}h_{\phi\nu}^* - \omega\epsilon e_{\rho\tau}e_{\rho\nu}^*)\,dl - \oint_c \tan\psi(\omega\mu h_{z\tau}h_{z\nu}^* \pm \omega\mu h_{\phi\tau}h_{\phi\nu}^* - \omega\epsilon e_{\rho\tau}e_{\rho\nu}^*)\,dl\right] \tag{18}$$

$$\kappa_{\tau\tau}^{-} = -\frac{1}{2}\left[\oint_o \tan\theta h_{\phi\rho}^* e_{\rho\tau}\,dl - \oint_c \tan\psi\, h_{\phi\tau}^* e_{\rho\tau}\,dl\right] - \frac{1}{2}\frac{1}{Z_\tau}\frac{dZ_\tau}{dz} \tag{19}$$

$$\kappa_{\tau\tau}^{+} = 0. \tag{20}$$

The coupling coefficients between TM_ν and TM_τ modes are

$$\kappa_{\nu\tau}^{\pm} = \frac{1}{2}\frac{1}{\beta_\nu \mp \beta_\tau}\left[\oint_o \tan\theta(\pm\omega\mu h_{\phi\tau}h_{\phi\nu}^* - \omega\epsilon e_{\rho\tau}e_{\rho\nu}^*)\,dl - \oint_c \tan\psi(\pm\omega\mu h_{\phi\tau}h_{\phi\nu}^* - \omega\epsilon e_{\rho\tau}e_{\rho\nu}^*)\,dl\right] \tag{21}$$

$$\kappa_{\tau\tau}^{-} = -\frac{1}{2}\left[\oint_o \tan\theta\, h_{\phi\tau}^* e_{\tau\tau}\,dl - \oint_c \tan\psi\, h_{\phi\tau}^* e_{\rho\tau}\,dl\right] - \frac{1}{2}\frac{1}{Z_\tau}\frac{dZ_\tau}{dz} \tag{22}$$

$$\kappa_{\tau\tau}^{+} = 0. \tag{23}$$

The coupling coefficients between TE_ν and TM_τ modes are

$$-\kappa_{\nu\tau}^{+} = \kappa_{\nu\tau}^{-} = \kappa_{\tau\nu}^{\pm *} = -\frac{1}{2}\left[\oint_o \tan\theta h_{\phi\tau}e_{\rho\nu}^*\,dl - \oint_c \tan\psi h_{\phi\tau}e_{\rho\nu}^*\,dl\right]. \tag{24}$$

The coupling coefficients between the TEM (denoted by subscript o) and TM_τ modes are

$$-\kappa_{o\tau}^{+} = \kappa_{o\tau}^{-} = \kappa_{\tau o}^{\pm *} = \frac{1}{2}\left[\oint_o \tan\theta\, h_{\phi\tau}e_{\rho o}^*\,dl - \oint_c \tan\psi h_{\phi\tau}e_{\rho o}^*\,dl\right]. \tag{25}$$

In the above equations, $\boldsymbol{e}_\tau(\rho, \phi)$ and $\boldsymbol{h}_\tau(\rho, \phi)$ are, respectively, the power normalized electric and magnetic fields which can be obtained from the normalized fields of Section II as follows:

$$\boldsymbol{e}_{t\tau} = \sqrt{Z_\tau}\tilde{\boldsymbol{e}}_{t\tau} \tag{26a}$$

$$e_{z\tau} = \frac{1}{j\omega\epsilon}\frac{1}{\sqrt{Z_\tau}}k_\tau \tilde{e}_{z\tau} \tag{26b}$$

$$\boldsymbol{h}_{t\tau} = \frac{1}{\sqrt{Z_\tau}}\tilde{\boldsymbol{h}}_{t\tau} \tag{26c}$$

$$h_{z\tau} = \frac{1}{j\omega\mu}\sqrt{Z_\tau}k_\tau \tilde{h}_{z\tau}. \tag{26d}$$

The fields above satisfy the power normalization

$$\int\int_{S_o} (\boldsymbol{e}_{t\tau} \times \boldsymbol{h}_{t\tau}^*) \cdot \hat{\boldsymbol{a}}_z\, dS = 1. \tag{27}$$

Furthermore, $\oint_o dl$ and $\oint_c dl$, respectively, denote line integrals along the boundary of the cross-section of the outer and center conductors.

IV. The Normal Modes of a Uniform Circular Coaxial Waveguide

To derive the explicit formulas for the coupling coefficients from (9)–(12), we need to obtain the expressions for the normalized eigenfields of a uniform circular coaxial waveguide. The eigenmodes of a uniform coaxial waveguide consist of TE_{mn}, TM_{mn}, and TEM modes. The indices m and n, where $m = 0, 1, 2, \cdots$ and $n = 1, 2, \cdots$ take the place of ν and τ in the previous sections. Here m identifies the number of periods of the fields in the azimuthal direction, and n denotes the number of half "periods" in the radial direction from $\rho = a$ to $\rho = b$. The radii of the center and outer conductors are designated by a and b, respectively.

TM_{mn} modes: The transverse components of the eigenfunctions, $\tilde{\boldsymbol{e}}_{[mn]}$ and $\tilde{\boldsymbol{h}}_{[mn]}$ (the bracket around the indices indicates a TM mode) for TM_{mn} modes can be obtained from the potential function

$$\Psi_{[mn]} = \frac{1}{R_{[mn]}} f_{mm}(k_{[mn]}\rho)\begin{Bmatrix}\sin(m\phi)\\ \cos(m\phi)\end{Bmatrix}, \tag{28}$$

[(14) and (A-13). Furthermore, $\tilde{e}_{z[mn]} = k_{[mn]}\Psi_{[mn]}$ and $\tilde{h}_{z[mn]} = 0$. The function $f_{mm}(k_{[mn]}\rho)$ is defined as

$$f_{mm}(k_{[mn]}\rho) = J_m(k_{[mn]}a)N_m(k_{[mn]}\rho) - N_m(k_{[mn]}a)J_m(k_{[mn]}\rho) \tag{29}$$

to simplify the notation. We also define $f_{mm'}(k_{[mn]}\rho)$ as follows for future reference:

$$f_{mm'}(k_{[mn]}\rho) = J_m(k_{[mn]}a)N_m'(k_{[mn]}\rho) - N_m(k_{[mn]}a)J_m'(k_{[mn]}\rho). \tag{30}$$

In (30), the prime on N_m or J_m denotes differentiation with respect to the argument of the function. Here, J_m is the Bessel function of the first kind of mth order, and N_m is the Bessel function of the second kind of mth order. Here $k_{[mn]}$ is the solution of the equation $f_{mm}(k_{[mn]}b) = 0$. The propagation constant $\beta_{[mn]}$ is obtained from

$$k_{[mn]}^2 + \beta_{[mn]}^2 = k^2 \tag{31}$$

and the normalization constant is

$$R_{[mn]} = \sqrt{\frac{\pi\epsilon_m}{2}}((k_{[mn]}b)^2 f_{mm'}^2(k_{[mn]}b) - (k_{[mn]}a)^2 f_{mm'}^2(k_{[mn]}a))^{1/2} \tag{32}$$

where

$$\epsilon_m = \begin{cases} 2 & \text{if } m = 0 \\ 1 & \text{if } m \neq 0. \end{cases} \tag{33}$$

The transverse wave impedance $Z_{[mn]}$ of a TM_{mn} mode is $\beta_{[mn]}/\omega\epsilon$.

TE_{mn} Modes: The transverse components of the eigenfunctions, $\tilde{\boldsymbol{e}}_{(mn)}$ and $\tilde{\boldsymbol{h}}_{(mn)}$, (the parentheses around the indices indicates a TE mode) of the TE_{mn} modes are obtained from the potential function

$$\Psi_{(mn)} = \frac{1}{R_{(mn)}} f_{m'm}(k_{(mn)}\rho)\begin{cases}\cos(m\phi) \\ \sin(m\phi)\end{cases} \tag{34}$$

(13) and (A-13). Furthermore, $\tilde{h}_{z(mn)} = k_{(mn)}\Psi_{(mn)}$ and $\tilde{e}_{z(mn)} = 0$. The auxiliary function $f_{m'm}(k_{(mn)}\rho)$ is defined as

$$f_{m'm}(k_{(mn)}\rho) = J'_m(k_{(mn)}a)N_m(k_{(mn)}\rho) - N'_m(k_{(mn)}a)J_m(k_{(mn)}\rho). \tag{35}$$

Here $k_{(mn)}$ is the solution of the equation

$$J'_m(k_{(mn)}a)N'_m(k_{(mn)}b) - N'_m(k_{(mn)}a)J'_m(k_{(mn)}b) = 0. \tag{36}$$

The propagation constant $\beta_{(mn)}$ is obtained from $k_{(mn)}^2 + \beta_{(mn)}^2 = k^2$ and the normalization constant $R_{(mn)}$ is

$$R_{(mn)} = \sqrt{\frac{\pi\epsilon_m}{2}}(((k_{(mn)}b)^2 - m^2)f_{m'm}^2(k_{(mn)}b) - ((k_{(mn)}a)^2 - m^2)f_{m'm}^2(k_{(mn)}a))^{1/2} \tag{37}$$

where ϵ_m is defined in (33). The transverse wave impedance of TE_{mn} mode is $\omega\mu/\beta_{(mn)}$.

TEM Mode: The normalized fields of the TEM mode can be shown to be

$$\tilde{e}_{\rho o} = \tilde{h}_{\phi o} = \frac{1}{R_o\rho} \tag{38}$$

where R_o (the subscript o indicates the TEM mode) is the normalization constant and its value is

$$R_o = \sqrt{2\pi}[\ln(b/a)]^{1/2}. \tag{39}$$

The wave impedance Z_o is $\sqrt{\mu/\epsilon}$, and the propagation constant β_o is $\omega\sqrt{\mu\epsilon}$.

V. The Explicit Formulas for the Coupling Coefficients

From the mode functions of the transverse electric fields of a uniform circular coaxial guide given in Section IV and the integral equations (9)–(12), explicit formulas for the coupling coefficients can be derived for the case of a varying-radius coaxial guide. We can make the following general statements with regard to the coupling coefficients for varying-radius perturbations.

1) Only modes with the same azimuthal index m couple to each other.
2) Only modes with the same polarization couple to each other.
3) TE_{0n} and TM_{0q} modes are not coupled to each other since if one is copolarized, the other is cross polarized.
4) The TEM mode is only coupled to TM_{0n} modes.

The coupling coefficients between TE_{mn} and TE_{mq} modes are

$$\kappa_{nq}^{\pm} = \frac{1}{2}\frac{\epsilon_m\pi}{R_{(mq)}R_{(mn)}}\frac{1}{k_{(mq)}^2 - k_{(mn)}^2} \cdot \left\{K_{nq}\sqrt{\frac{\beta_{(mn)}}{\beta_{(mq)}}} \pm K_{qn}\sqrt{\frac{\beta_{(mq)}}{\beta_{(mn)}}}\right\} \tag{40}$$

when $n \neq q$. Here

$$K_{nq} = k_{(mq)}^2\left\{\frac{1}{b}\frac{db}{dz}((k_{(mn)}b)^2 - m^2) \cdot f_{m'm}(k_{(mn)}b)f_{m'm}(k_{(mq)}b) - \frac{1}{a}\frac{da}{dz}((k_{(mn)}a)^2 - m^2)f_{m'm}(k_{(mn)}a) \cdot f_{m'm}(k_{(mq)}a)\right\}. \tag{41}$$

When $n = q$, then $\kappa_{nn}^{+} = 0$ and

$$\kappa_{nn}^{-} = -\frac{\pi\epsilon_m}{2}\frac{m^2}{R_{(mn)}^2}\left\{\frac{1}{b}\frac{db}{dz}f_{m'm}^2(k_{(mn)}b) - \frac{1}{a}\frac{da}{dz}f_{m'm}^2(k_{(mn)}a)\right\} - \frac{1}{2}\frac{1}{\beta_{(mn)}^2}k_{(mn)}\frac{dk_{(mn)}}{dz} \tag{42}$$

$$\frac{dk_{(mn)}}{dz} = -k_{(mn)} \times \frac{(k_{(mn)}b)^2[(k_{(mn)}a)^2 - m^2]f_{mm'}(k_{(mn)}b)\frac{da}{dz} + (k_{(mn)}a)^2[(k_{(mn)}b)^2 - m^2]f_{m'm}(k_{(mn)}b)\frac{db}{dz}}{(k_{(mn)}b)^2[(k_{(mn)}a)^2 - m^2]f_{mm'}(k_{(mn)}b)a + (k_{(mn)}a)^2[(k_{(mn)}b)^2 - m^2]f_{m'm}(k_{(mn)}b)b} \tag{43}$$

where $dk_{(mn)}/dz$) is (see (43), shown at the bottom of the previous page).

The coupling coefficients between TM_{mn} and TM_{mq} modes are

$$\kappa_{nq}^{\pm} = \frac{1}{2}\frac{\pi\epsilon_m}{R_{[mn]}R_{[mq]}}\frac{k_{[mn]}k_{[mq]}}{k_{[mq]}^2 - k_{[mn]}^2} \times K \times \left\{ k_{[mn]}^2\sqrt{\frac{\beta_{[mq]}}{\beta_{[mn]}}} \pm k_{[mq]}^2\sqrt{\frac{\beta_{[mn]}}{\beta_{[mq]}}} \right\} \quad (44)$$

when $n \neq q$. Here we have

$$K = f_{mm'}(k_{[mn]}b)f_{mm'}(k_{[mq]}b)b\frac{db}{dz} - f_{mm'}(k_{[mn]}a)f_{mm'}(k_{[mq]}a)a\frac{da}{dz}. \quad (45)$$

When $n = q$, then $\kappa_{nn}^{+} = 0$ and

$$\kappa_{nn}^{-} = -\frac{\pi\epsilon_m}{2}\frac{k_{[mn]}^2}{R_{[mn]}^2}\left(bf_{mm'}^2(k_{[mn]}b)\frac{db}{dz} - af_{mm'}^2(k_{[mn]}a)\frac{da}{dz}\right) - \frac{1}{2}\frac{k_{[mn]}^2}{\beta_{[mn]}^2}\frac{f_{mm'}(k_{[mn]}b)\frac{db}{dz} + f_{m'm}(k_{[mn]}b)\frac{da}{dz}}{bf_{mm'}(k_{[mn]}b) + af_{m'm}(k_{[mn]}b)}. \quad (46)$$

The coupling coefficients between TE_{mn} and TM_{nq} modes are

$$-\kappa_{nq}^{+} = \kappa_{nq}^{-} = \kappa_{qn}^{\pm} = \frac{1}{2}\frac{\pi m}{R_{(mn)}R_{[mq]}}\frac{k_{[mq]}k}{\sqrt{\beta_{(mn)}\beta_{[mq]}}} \times \left\{ f_{m'm}(k_{(mn)}b)f_{mm'}(k_{[mq]}b)\frac{db}{dz} - f_{m'm}(k_{(mn)}a)f_{mm'}(k_{[mq]}a)\frac{da}{dz}\right\}. \quad (47)$$

The coupling coefficients between the TEM mode and TM_{0n} modes are

$$\kappa_{no}^{\pm} = -\kappa_{on}^{+} = \kappa_{on}^{-} = \frac{\pi k_{[0n]}}{R_o R_{[0n]}}\sqrt{\frac{\beta_o}{\beta_{[0n]}}}\left(f_{00'}(k_{[0n]}b)\frac{db}{dz} - f_{00'}(k_{[0n]}a)\frac{da}{dz}\right). \quad (48)$$

The coupling coefficients between the forward and backward propagating TEM modes are

$$\kappa_{oo}^{+} = 0 \quad (49)$$

$$\kappa_{oo}^{-} = -\frac{\pi}{R_o^2}\left(\frac{1}{b}\frac{db}{dz} - \frac{1}{a}\frac{da}{dz}\right). \quad (50)$$

VI. Discussion of the Method of Cross Sections

The coupled mode equations (8) are valid for the description of nonuniform waveguides with a slowly varying cross section. This is because the use of the transformation (7) restricts us to propagating modes. Hence, in the formulation represented by (8), it is assumed that the fields in the nonuniform guide can be represented correctly by only the propagating modes, and the evanescent modes are neglected. However, in nonuniform waveguides with slowly varying cross sections, the evanescent modes are rarely excited to any appreciable level [14], [20]. Hence, including only propagating modes is usually sufficient. Huting and Webb [21] have shown that it is not necessary to require the slowly varying constraint if, in addition to propagating modes, evanescent modes are considered in the calculation by using the voltage-current formulation (A-17) and (A-18). In the voltage-current formulation, the coupling coefficient is $C_{\nu\tau}$ given by (12) instead of $\kappa_{\nu\tau}$.

In order to apply the method of cross sections to more rapidly varying cross sections where the evanescent modes are not considered, we can approximate the wall of the nonuniform guide at $z = z_o$ with a uniform conical section where the slope of the conical section is the same as that of the nonuniform guide at $z = z_o$. For the infinite series representation of the fields of the nonuniform guide, we then employ the normal modes of the uniform round conical coaxial guide. In this case, the infinite series converges uniformly. The possible drawback would be that the coupling coefficients might be considerably more complicated, and may not be suitable for analysis and synthesis of irregular waveguides. The coupling coefficients between the conical TE_{0n} modes of a slowly varying radius hollow circular guide have been derived by Sporleder and Unger [14]. In the present paper, we assume waveguides with a slowly varying cross section, so cylindrical model functions are used.

VII. Discussion of the Coupling Coefficients

Let us write the expression for the coupling coefficient from mode mq to mode mn in the following form:

$$\kappa_{nq}^{\pm} = \tilde{\kappa}_{nq,\,o}^{\pm}\frac{db}{dz} + \tilde{\kappa}_{nq,\,c}^{\pm}\frac{da}{dz} \quad (51)$$

where $\tilde{\kappa}_{nq,\,o}^{\pm}$ will be referred to as the coupling factor for the outer conductor and $\tilde{\kappa}_{nq,\,c}^{\pm}$ as the coupling factor for the center conductor. In this section, some computational plots of the coupling factors between modes propagating in the same direction, i.e., $\tilde{\kappa}_{nq,\,o}^{+}$ and $\tilde{\kappa}_{nq,\,c}^{+}$, will be given.

The expressions for the field components in Section IV are chosen such that the signs of the radial function of any of the field components e_ρ, h_ϕ, or h_z are the same at the center conductor. These field components for TE_{mn} and TM_{mn} modes then alternate in sign with increasing or decreasing n at the outer wall. This is shown in Fig. 2 for the case of the longitudinal component of magnetic field, h_z, for TE_{0n} modes.

The sign of the coupling factor depends on the signs of the fields at the walls. Specifically, the signs of the coupling factors for the center conductor are the same from the TE_{01} mode to higher-order TE_{0n} modes, while these coupling

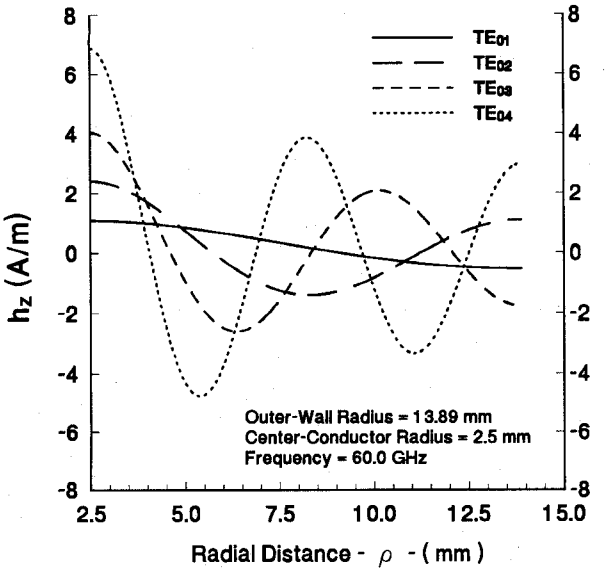

Fig. 2. The variation in the longitudinal component of magnetic fields of four of TE_{0n} modes in the cross section of a coaxial waveguide.

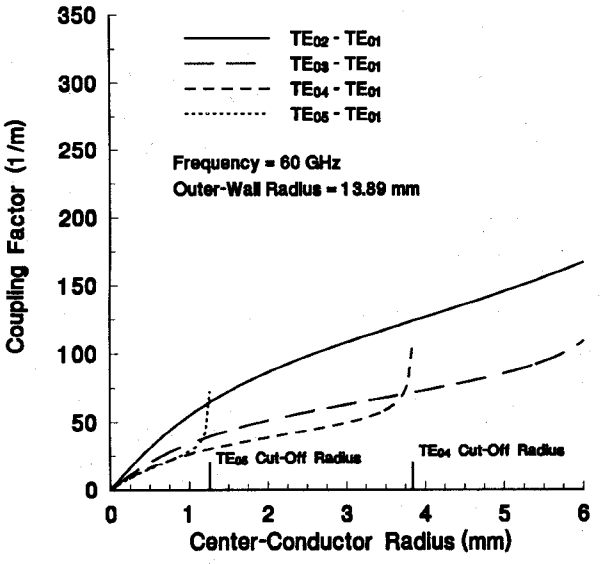

Fig. 3. The coupling factor for the center conductor between the TE_{01} and four higher-order TE_{0n} modes as a function of the center-conductor radius.

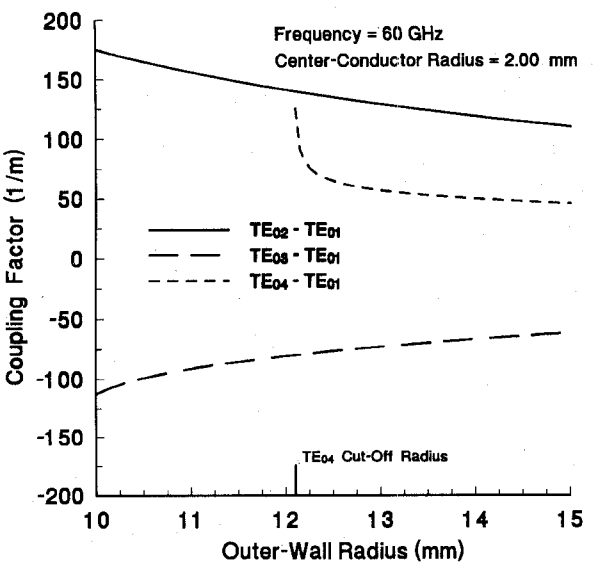

Fig. 4. The coupling factor for the outer wall between the TE_{01} and three higher-order TE_{0n} modes as a function of the outer-conductor radius.

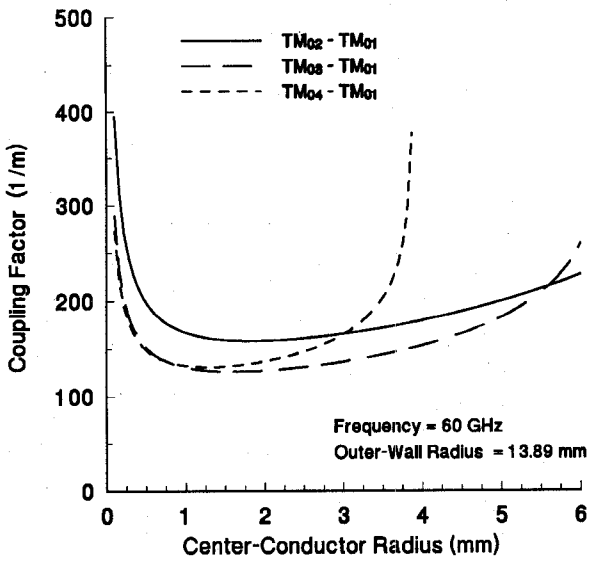

Fig. 5. The coupling factor for the center conductor between the TM_{01} and three higher-order TM_{0n} modes as a function of the center-conductor radius.

factors for the outer wall alternate in sign. This is illustrated in Fig. 3 where we have plotted the coupling factors for the center conductor as a function of the center-conductor radius. Fig. 4 shows the coupling factors for the outer conductor as a function of the outer-conductor radius.

By letting the radius of the center conductor become vanishingly small, i.e., when $a \rightarrow 0$, and by using the small argument expressions for the Bessel functions, one can show that the coupling factors for the center conductor vanish, except for the case of TM_{0n} modes and the TEM mode (which are discussed below), while the coupling coefficients due to the outer-wall radius variation converge to those of a hollow circular guide with a varying-radius wall. These hollow waveguide coupling coefficients have already been derived by others [15], [16].

For TM_{0n} modes, as the radius of the center conductor becomes small, the center conductor behaves like a line charge. The transverse fields, E_ρ and H_ϕ, of TM_{0n} modes become very large at the surface of the inner conductor, and hence the coupling factors for the center conductor between TM_{0n} modes diverge as the radius of the center conductor decreases. In the center of a hollow circular guide, E_z is maximum for TM_{0n} modes, but a conducting line at the center forces the longitudinal field E_z to become zero. Three of the coupling factors for the center conductor from TM_{01} to TM_{0n} modes have been plotted in Fig. 5 as a function of the center-conductor radius. Between TM_{mn} modes with $m \neq 0$, the coupling factors for the center conductor tend to zero as the inner-conductor radius vanishes. The longitudinal electric field at the center of a hollow circular guide is zero for these modes.

The coupling factors for the inner conductor between the TEM and TM_{0n} modes also diverge as the radius of the center conductor tends to zero. The coupling factors for the outer wall between these modes vanish as $a \rightarrow 0$.

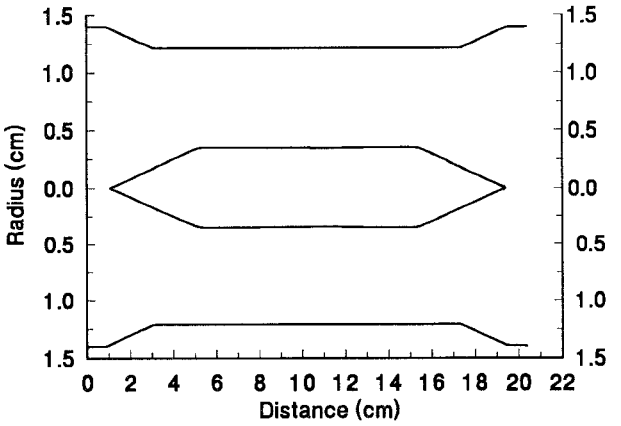

Fig. 6. The profile of the center and outer conductors of the coaxial waveguide used in the experimental study of the coupling coefficients between TE_{0n} modes.

For rotating modes with $\exp(-jm\phi)$ or $\exp(jm\phi)$ dependence instead of stationary modes with $\cos(m\phi)$ or $\sin(m\phi)$ dependence, $\epsilon_m = 2$ for all m instead of (33). The coupling coefficients (40)–(50) are still valid for rotating modes since, on closer examination, we observe that the coupling coefficients are not dependent on ϵ_m.

VIII. Experimental Results

In this section, we report on the experimental results of mode conversion for the azimuthally symmetric transverse electric modes (the TE_{0n} modes) at 60 GHz in a coaxial waveguide in which the radius of both the center and outer conductors vary. The varying-radius coaxial guide designed for this experiment, shown in Fig. 6, is composed of two identical tapered sections with a uniform section of waveguide in between. The angle that both the inner and outer conductor tapers make with the z-axis is 5°. The diameter of the outer conductor at the ends in 2.779 cm, and the diameters of the uniform center and outer conductors in between the tapered sections are 0.721 cm and 2.423 cm, respectively. The lengths of the center- and outer-conductor tapered sections are, respectively, 4.115 cm and 2.032 cm.

The coupled mode equations (8) for the forward-propagating TE_{0n} modes were numerically integrated along the varying-radius coaxial waveguide. The input is assumed to be a pure TE_{01} mode with unit power. The length of the uniform section is chosen to maximize the amount of mode conversion from the TE_{01} mode to the TE_{02} mode. The computed amplitude of TE_{01} mode and the coupled higher-order TE_{0n} modes along the guide are plotted in Fig. 7. The TE_{04} and TE_{05} modes are evanescent in the small-diameter region of the waveguide. They were included in the calculation in the region in which they can propagate in order to ascertain that coupling to them was negligible. The ohmic losses were included in the calculation.

The mode conversion efficiencies were measured at low power level. This was done by feeding a TE_{01} mode into one end and measuring the E_ϕ component of the far-field radiation pattern from the output end. The mode content of each of the TE_{0n} modes present can be determined to within about 2% from this open-end radiation pattern [17]. The center conductor

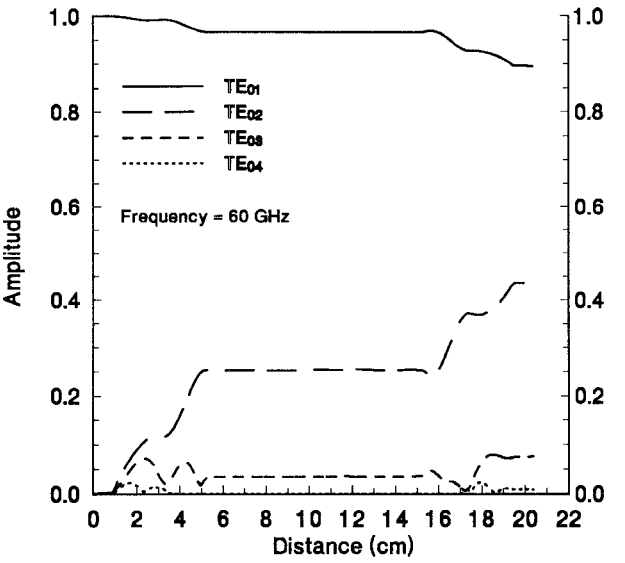

Fig. 7. The theoretical amplitudes of the incident TE_{01} mode and the coupled TE_{0n} modes along the varying-radius coaxial waveguide of Fig. 6.

was supported by two thin styrofoam dielectric cylinders with a dielectric constant of about 1.03. Experiment showed that the mode conversion level from TE_{01} to TE_{02} decreases slightly as the styrofoam sections were made longer. Hence, here the effect of the supporting styrofoam sections is to lower the mode conversion. In the computational results presented in this section, the effect of the styrofoam is not accounted for, but is believed to be small.

The circular waveguide TE_{01} mode input into the varying-radius coaxial guide was obtained by using a mode transducer which converts a rectangular waveguide TE_{10} mode to a circular waveguide TE_{01} mode followed by a circular waveguide mode filter, both of which are commercially available (from Alpha-TRG). The circular waveguide diameter of these devices was only 0.968 cm, so a special up-taper was designed to taper to the necessary 2.779 cm diameter. The radiation pattern was measured with a 1.65 m rotating arm on which a small receiving horn was mounted. The signal was detected using a superheterodyne receiver. The comparison between the measured and computed E_ϕ component of the far-field radiation patterns of the TE_{01} mode is shown in Fig. 8. The TE_{01} mode at the 2.779 cm end has a mode purity of greater than 99%.

In Fig. 9, the E_ϕ component of the measured far-field radiation pattern output from the varying-radius coaxial guide is compared to the E_ϕ pattern resulting from the computed amplitudes of the modes at the output. The agreement is good. The measured E_ϕ radiation pattern of the input TE_{01} mode is also plotted in this figure. The measured and computed power levels of the TE_{0n} modes with significant amplitudes at the output are listed in row 3 of Table I. The data in the first row of this table correspond to a coaxial guide having a uniform outer wall with a diameter of 2.779 cm and a center conductor with the same radius profile as that for the coaxial guide shown in Fig. 6. The data in row 2 correspond to a hollow waveguide with the same radius profile as that of the outer wall of the coaxial guide shown in Fig. 6.

TABLE I
PERCENT MODAL POWER AT THE END OF THE COAXIAL WAVEGUIDE

	Theory			Measurement		
	TE_{01}	TE_{02}	TE_{03}	TE_{01}	TE_{02}	TE_{03}
Varying–Radius Center Cond. Outer–Wall Diameter = 2.778 cm	90.89	8.91	0.20	92.23	7.66	0.11
Varying–Radius Outer Cond. (Hollow Guide)	86.89	12.61	0.50	90.95	8.78	0.27
Varying–Radius Center Cond. Varying–Radius Outer Cond.	80.26	19.14	0.60	83.16	16.80	0.04

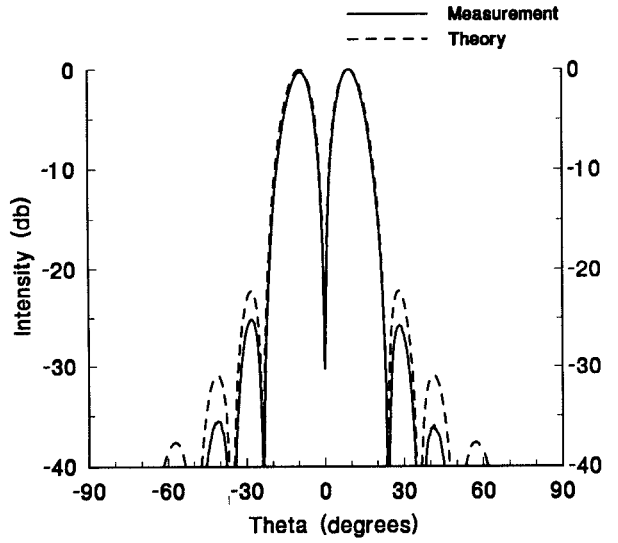

Fig. 8. The measured and computer far-field radiation patterns of the TE_{01} mode which was the input into the varying-radius coaxial guide of Fig. 6.

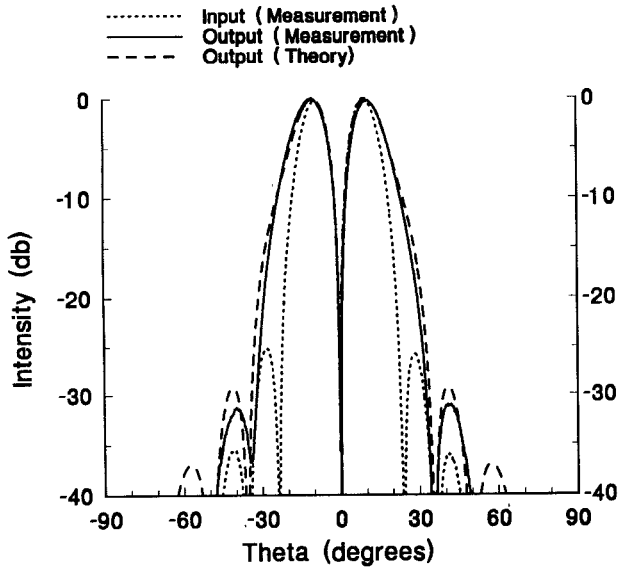

Fig. 9. The measured and computed far-field radiation patterns of mode mixtures at the output end of the varying-radius coaxial guide of Fig. 6. The input mode is the TE_{01} mode.

The discrepancy between the measured and theoretical results might be due to one or more of the following mode conversion mechanisms that are not accounted for in our computational results. 1) The transition regions between the tapered and the straight sections of the coaxial waveguide are abrupt, as seen in Fig. 6. In these sharp regions, the coupling coefficients are not valid. 2) It is difficult to center the center conductor precisely. 3) There is also some undesired mode conversion due to the misalignment of the different waveguide sections that were used in the experimental setup.

IX. CONCLUSION

We have derived the explicit formulas for the coupling coefficients in a varying-radius coaxial waveguide, and discussed the signs of the coupling coefficients for the center and outer conductors. A simple coaxial tapered section, where both the inner and outer radii vary, was designed to check for TE_{0n} modes, the coupling coefficients, and particularly their relative signs at the guide walls. The experimental results show reasonable agreement with theory, and clearly show the sign convention is correct. By letting the radius of the center conductor become vanishingly small, the coupling coefficients due to outer wall variations agree with those of a hollow circular guide with a varying radius.

X. APPENDIX I
DERIVATION OF THE COUPLED DIFFERENTIAL EQUATIONS

Below, we briefly sketch the derivation of the coupled differential equations for the propagating modes that appear in (8)–(12). These equations were originally obtained by Reiter [18] and Solymar [13] for the case of nonuniform hollow waveguides.

We define the inner product between two scalar functions u_1 and u_2 over the waveguide cross section S_o by

$$\langle u_1, u_2 \rangle = \int\int_{S_o} u_1 u_2^* \, dS \tag{A1}$$

where $*$ indicates the complex conjugate of the function.

Our goal is to derive a system of coupled differential equations describing the complex coefficients V_τ and I_τ of the infinite series expansion (4). Maxwell's curl equations for the total fields in the waveguide in the cylindrical coordinate system are

$$\frac{1}{\rho}\frac{\partial}{\partial \phi} E_z - \frac{\partial}{\partial z} E_\phi = -j\omega\mu H_\rho \tag{A2a}$$

$$\frac{\partial}{\partial z}E_\rho - \frac{\partial}{\partial \rho}E_z = -j\omega\mu H_\phi \tag{A2b}$$

$$\frac{1}{\rho}\frac{\partial}{\partial \rho}(\rho E_\phi) - \frac{1}{\rho}\frac{\partial}{\partial \phi}E_\rho = -j\omega\mu H_z \tag{A2c}$$

$$\frac{1}{\rho}\frac{\partial}{\partial \phi}H_z - \frac{\partial}{\partial z}H_\phi = j\omega\epsilon E_\rho \tag{A2d}$$

$$\frac{\partial}{\partial z}H_\rho - \frac{\partial}{\partial \rho}H_z = j\omega\epsilon E_\phi \tag{A2e}$$

$$\frac{1}{\rho}\frac{\partial}{\partial \rho}(\rho H_\phi) - \frac{1}{\rho}\frac{\partial}{\partial \phi}H_\rho = j\omega\epsilon E_z. \tag{A2f}$$

Starting from (A2a), and taking its inner product with $\tilde{e}_{\phi\nu}$ over S_o, we have

$$\left\langle \frac{1}{\rho}\frac{\partial}{\partial \phi}E_z,\, \tilde{e}_{\phi\nu} \right\rangle - \left\langle \frac{\partial}{\partial z}E_\phi,\, \tilde{e}_{\phi\nu} \right\rangle = -j\omega\mu\langle H_\rho,\, \tilde{e}_{\phi\nu}\rangle. \tag{A3}$$

The series expansion (4) of the fields converges in the mean-square sense, but term-by-term differentiation of the infinite series requires stronger convergence. Hence, in general, we cannot take the differential operators inside the sum. Therefore, to avoid this difficulty, we use integration by parts to transfer the differential operators to the second term of the inner product.

Applying integration by parts and noting that $\tilde{e}_{\phi\nu}$ vanishes at the wall of the guide, the first inner product in (A3) becomes

$$\left\langle \frac{1}{\rho}\frac{\partial}{\partial \phi}E_z,\, \tilde{e}_{\phi\nu} \right\rangle = -\left\langle E_z,\, \frac{1}{\rho}\frac{\partial}{\partial \phi}\tilde{e}_{\phi\nu} \right\rangle \tag{A4}$$

and the second inner product yields

$$\left\langle \frac{\partial}{\partial z}E_\phi,\, \tilde{e}_{\phi\nu} \right\rangle = \frac{\partial}{\partial z}\langle E_\phi,\, \tilde{e}_{\phi\nu}\rangle - \left\langle E_\phi,\, \frac{\partial}{\partial z}\tilde{e}_{\phi\nu} \right\rangle. \tag{A5}$$

Equation (A3) hence reduces to

$$-\left\langle E_z,\, \frac{1}{\rho}\frac{\partial}{\partial \phi}\tilde{e}_{\phi\nu} \right\rangle - \frac{\partial}{\partial z}\langle E_\phi,\, \tilde{e}_{\phi\nu}\rangle + \left\langle E_\phi,\, \frac{\partial}{\partial z}\tilde{e}_{\phi\nu} \right\rangle = -j\omega\mu\langle H_\rho,\, \tilde{e}_{\phi\nu}\rangle. \tag{A6}$$

We then substitute the infinite series representation of the fields into (A6), and interchange the order of summation and integration since the inner product is a continuous function of its argument [19]. We thus have

$$-\sum_\tau v_\tau \left\langle \tilde{e}_{z\tau},\, \frac{1}{\rho}\frac{\partial}{\partial \phi}\tilde{e}_{\phi\nu} \right\rangle - \frac{\partial}{\partial z}\sum_\tau V_\tau\langle \tilde{e}_{\phi\tau},\, \tilde{e}_{\phi\nu}\rangle + \sum_\tau V_\tau \left\langle \tilde{e}_{\phi\tau},\, \frac{\partial}{\partial z}\tilde{e}_{\phi\nu} \right\rangle = -j\omega\mu\sum_\tau I_\tau\langle \tilde{h}_{\rho\tau},\, \tilde{e}_{\phi\nu}\rangle. \tag{A7}$$

Next, we take the inner product of (A2b) with $\tilde{e}_{\rho\nu}$ to obtain

$$\left\langle \frac{\partial}{\partial z}E_\rho,\, \tilde{e}_{\rho\nu} \right\rangle - \left\langle \frac{\partial}{\partial \rho}E_z,\, \tilde{e}_{\rho\nu} \right\rangle = -j\omega\mu\langle H_\phi,\, \tilde{e}_{\rho\nu}\rangle. \tag{A8}$$

Once again, by transferring the differential operators to the second term in the inner products, we have

$$\left\langle \frac{\partial}{\partial z}E_\rho,\, \tilde{e}_{\rho\nu} \right\rangle = \frac{\partial}{\partial z}\langle E_\rho,\, \tilde{e}_{\rho\nu}\rangle - \left\langle E_\rho,\, \frac{\partial}{\partial z}\tilde{e}_{\rho\nu} \right\rangle - \oint_o \tilde{e}^*_{\rho\nu}E_\rho \tan\theta\, dl + \oint_c \tilde{e}^*_{\rho\nu}E_\rho \tan\psi\, dl \tag{A9}$$

$$\left\langle \frac{\partial}{\partial \rho}E_z,\, \tilde{e}_{\rho\nu} \right\rangle = -\left\langle E_z,\, \frac{1}{\rho}\tilde{e}_{\rho\nu} \right\rangle - \left\langle E_z,\, \frac{\partial}{\partial \rho}\tilde{e}_{\rho\nu} \right\rangle + \oint_o \tilde{e}^*_{\rho\nu}E_z\, dl - \oint_c \tilde{e}^*_{\rho\nu}E_z\, dl \tag{A10}$$

where $\oint_o$ and $\oint_c$, respectively, denote line integrals along the boundary of the outer and center conductors. The line integrals in (A9) arise to take into account the change in the cross section of the guide in the z-direction. By substituting the last two equations into (A8), we then obtain

$$\frac{\partial}{\partial z}\langle E_\rho,\, \tilde{e}_{\rho\nu}\rangle - \left\langle E_\rho,\, \frac{\partial}{\partial z}\tilde{e}_{\rho\nu} \right\rangle + \left\langle E_z,\, \frac{1}{\rho}\tilde{e}_{\rho\nu} \right\rangle + \left\langle E_z,\, \frac{\partial}{\partial \rho}\tilde{e}_{\rho\nu} \right\rangle = -j\omega\mu\langle H_\phi,\, \tilde{e}_{\rho\nu}\rangle. \tag{A11}$$

The line integrals cancel each other due to the boundary conditions (2b) and (3b). Using the infinite series representation (4) in (A11) and interchanging the order of summation and integration, we obtain the following:

$$\frac{\partial}{\partial z}\sum_\tau V_\tau\langle \tilde{e}_{\rho\tau},\, \tilde{e}_{\rho\nu}\rangle - \sum_\tau V_\tau \left\langle \tilde{e}_{\rho\tau},\, \frac{\partial}{\partial z}\tilde{e}_{\rho\nu} \right\rangle + \sum_\tau v_\tau \left\langle \tilde{e}_{z\tau},\, \frac{1}{\rho}\tilde{e}_{\rho\nu} \right\rangle + \sum_\tau v_\tau \left\langle \tilde{e}_{z\tau},\, \frac{\partial}{\partial \rho}\tilde{e}_{\rho\nu} \right\rangle = -j\omega\mu\sum_\tau I_\tau\langle \tilde{h}_{\phi\tau},\, \tilde{e}_{\rho\nu}\rangle. \tag{A12}$$

We then combine (A7) and (A12) and use the orthogonality property of (5a) and also the relations

$$\tilde{\boldsymbol{h}}_{t\tau} = \hat{\boldsymbol{a}}_z \times \tilde{\boldsymbol{e}}_{t\tau} \tag{A13}$$

$$\langle \tilde{e}_{z\tau},\, \nabla_t \cdot \tilde{\boldsymbol{e}}_{t\nu}\rangle = k_\nu\, \delta_{\nu\tau} \tag{A14}$$

to obtain

$$\frac{d}{dz}V_\nu + k_\nu v_\nu - \sum_\tau V_\tau \int\int_{S_o} \tilde{\boldsymbol{e}}_{t\tau}\cdot\frac{\partial}{\partial z}\tilde{\boldsymbol{e}}^*_{t\nu}\, dS = -j\omega\mu I_\nu. \tag{A15}$$

Here, k_ν is the cutoff wavenumber of mode ν.

We can also find the following relation between v_ν and I_τ by taking the inner product of (A2f) with $\tilde{e}_{z\nu}$

$$v_\nu = \frac{k_\nu}{j\omega\varepsilon}I_\nu. \tag{A16}$$

Finally, by substituting the last equation into (A15), we establish the first set of coupled differential equations as follows:

$$\frac{dV_\nu}{dz} = -jZ_\nu\beta_\nu I_\nu + \sum_\tau V_\tau \int\int_{S_o} \tilde{\boldsymbol{e}}_{t\tau}\cdot\frac{\partial}{\partial z}\tilde{\boldsymbol{e}}^*_{t\nu}\, dS. \tag{A17}$$

Here, Z_ν is the transverse wave impedance of the mode with index ν.

The second set of coupled differential equations are derived from (A2d) and (A2e). Specifically, we first take the inner product of (A2d) with $\tilde{h}_{\phi\nu}$ and then the inner product of (A2e)

with $\tilde{h}_{\rho\nu}$, and combine the two to obtain the desired second set of coupled differential equations

$$\frac{dI_\nu}{dz} = -j\frac{\beta_\nu}{Z_\nu}V_\nu - \sum_\tau I_\tau \int\int_{S_o} \tilde{\boldsymbol{h}}^*_{t\nu} \cdot \frac{\partial}{\partial z}\tilde{\boldsymbol{h}}_{t\tau}\, dS. \qquad \text{(A18)}$$

The system of coupled differential equations (A17) and (A18) completely describes the coupling of modes in terms of the modal voltage V_ν and modal current I_ν in the nonuniform guide.

For our purposes it is convenient to write the coupled equations, not in terms of the modal voltage and current but in terms of the amplitudes of forward and backward propagating modes. The relation between these two formalisms is given in (7). If V_ν and I_ν in (A17) and (A18) are represented in terms of A^+_ν and A^-_ν, we obtain the coupled mode equations (8) for the forward and backward propagating modes in a varying-radius coaxial guide.

XI. Appendix II

By using the Bessel function Wronskians and vanishing of (29) and (36) at $\rho = b$, simplified expressions can be obtained for the following terms:

$$f_{mm'}(k_{[mn]}b) = \frac{2}{\pi(k_{[mn]}b)}\frac{J_m(k_{[mn]}a)}{J_m(k_{[mn]}b)} \qquad \text{(B1)}$$

$$f_{mm'}(k_{[mn]}a) = \frac{2}{\pi(k_{[mn]}a)} \qquad \text{(B2)}$$

$$f_{m'm}(k_{(mn)}b) = -\frac{2}{\pi(k_{(mn)}b)}\frac{J'_m(k_{(mn)}a)}{J'_m(k_{(mn)}b)} \qquad \text{(B3)}$$

$$f_{m'm}(k_{(mn)}a) = -\frac{2}{\pi(k_{(mn)}a)}. \qquad \text{(B4)}$$

References

[1] M. E. Read, G. S. Nusinovich, O. Dumbrajs, K. Kreischer, B. Levush, and G. Bird, "Design of a 3-megawatt, 140 GHz gyrotron with a coaxial cavity," in *17th Int. Conf. Infrared Millimeter Waves Dig.*, Pasadena, CA, Dec. 1992, pp. 192–193.

[2] S. N. Vlasov, L. I. Zagryadskaya, and I. M. Orlova, "Open coaxial resonators for gyrotrons," *Radio Eng. Electron. Phys.*, vol. 21, no. 7, pp. 96–102, 1976.

[3] P. J. Castro, J. J. Barroso, and R. A. Correa, "Cold tests of open coaxial resonators in the range of 9–17 GHz," *Int. J. Infrared Millimeter Waves*, vol. 14, no. 2, pp. 383–395, Feb. 1993.

[4] C. Moeller, "A coupled cavity whispering-gallery mode transducer," in *17th Int. Conf. Infrared Millimeter Waves Dig.*, Pasadena, CA, Dec. 1992, pp. 42–43.

[5] J. Shafii and R. J. Vernon, "Mode coupling in varying-radius coaxial waveguides," in *17th Int. Conf. Infrared Millimeter Waves Dig.*, Pasadena, CA, Dec. 1992, pp. 38–39.

[6] H. G. Unger, "Circular waveguide taper of improved design," *Bell Syst. Tech. J.*, pp. 899–912, July 1958.

[7] S. R. Seshadri, "Cylindrical waveguide mode converter for aximuthally symmetric transverse electric modes," *IEE Proc.*, vol. 135, Pt. H, no. 6, pp. 420–425, Dec. 1988.

[8] N. P. Kerzhentseva, "Conversion of wave modes in a waveguide with smoothly varying impedance of the walls," *Radio Eng. Electron. Phys.*, vol. 16, no. 1, pp. 24–31, 1971.

[9] H. Li and M. Thumm, "Mode coupling in corrugated waveguides with varying radius wall and diameter change," *Int. J. Electron.*, vol. 71, no. 5, pp. 827–844, 1991.

[10] B. Z. Katsenelenbaum, "On the theory of irregular acoustic waveguides," *Sov. Phys. Acoust.*, vol. 7, no. 2, pp. 159–164, Oct.–Dec. 1961.

[11] S. P. Morgan, "Theory of curved waveguides containing an inhomogeneous dielectric," *Bell Syst. Tech. J.*, pp. 1209–1251, Sept. 1957.

[12] R. F. Harrington, *Time-Harmonic Electromagnetic Fields*. New York: McGraw-Hill, 1961, ch. 5.

[13] L. Solymar, "Spurious mode generation in nonuniform waveguide," *IRE Trans. Microwave Theory Tech.*, pp. 379–383, 1959.

[14] F. Sporleder and H. G. Unger, *Waveguide Tapers, Transitions and Couplers*. London: Peregrinus, 1979.

[15] J. L. Doane, "Propagation and mode coupling in corrugated and smooth-wall circular waveguides," *Int. J. Infrared Millimeter Waves*, vol. 13, pp. 123–170, 1985.

[16] W. G. Lawson, "Theoretical evaluation of nonlinear tapers for a high power gyrotrons," *IEEE Trans. Microwave Theory Tech.*, vol. 38, pp. 1617–1622, Nov. 1990.

[17] R. J. Vernon, W. R. Pickels, M. J. Buckley, F. Firouzbakht, and J. A. Lorbeck, "Mode content determination in overmoded circular waveguides by open-end radiation pattern measurement," in *IEEE Int. Symp. Antennas Propagat. Dig.*, Blacksburg, VA, June 1987, pp. 222–225.

[18] G. Reiter, "Generalized telegraphists's equation for waveguides of varying cross section," *Inst. Elec. Eng.*, Paper 3028E, pp. 54–57, Sept. 1959.

[19] Ivar Stakgold, *Green's Functions and Boundary Value Problems*. New York: Wiley, 1979, ch. 4.

[20] W. A. Huting and K. J. Webb, "Numerical solution of the continuous waveguide transition problem," *IEEE Trans. Microwave Theory Tech.*, vol. MTT-37, pp. 1802–1808, 1989.

[21] ——, "Comparison of mode-matching and differential equation techniques in the analysis of waveguide transitions," *IEEE Trans. Microwave Theory Tech.*, vol. 39, pp. 280–286, 1991.

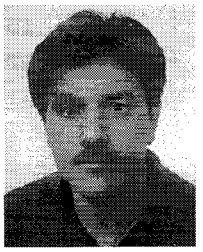

Jamal Shafii (S'89) received the B.S. degree from the University of Illinois at Urbana-Champaign, and the M.S. and Ph.D. degrees from the University of Wisconsin at Madison, all in electrical engineering.

His topics of graduate research included mode coupling in overmoded nonuniform waveguides and optimal design of mode converters and waveguide tapers.

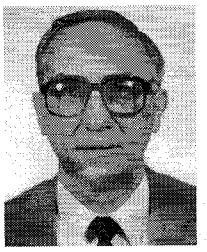

Ronald J. Vernon (S'64–M'65) was born in Chicago, IL, on June 3, 1936. He received the B.S., M.S., and Ph.D. degrees in electrical engineering from Northwestern University, Evanston, IL, in 1959, 1961, and 1965 respectively.

He worked under a cooperative student program in the Remote Control Engineering Division of Argonne National Laboratory from 1955 to 1958. Later he worked during the summer as an electrical engineer for the Communications and Industrial Electronics Division of Motorola Inc. Since 1965 he has been on the Faculty of the University of Wisconsin, Madison, where he is presently a professor of electrical and computer engineering. In 1976–1977 he took a leave of absence to work at Lawrence Livermore National Laboratory. His current research interests are in the development of transmission and mode conversion systems for high-power microwave tubes such as gyrotrons.

Dr. Vernon is a member of Sigma Xi, Tau Beta Pi, Eta Kappa Nu, and Pi Mu Epsilon.